# RADIATIVELY DRIVEN WINDS IN WOLF-RAYET STARS: A UNIFIED CORE-ATMOSPHERE MODEL

ROBERTO TUROLLA
International School for Advanced Studies, Trieste[1]

LUCIANO NOBILI
Department of Physics, University of Padova

AND

MASSIMO CALVANI
Department of Astronomy, University of Padova

## ABSTRACT

A sequence of chemically homogeneous, dynamical stellar models is constructed for different masses. Each model is computed by fitting onto a helium-burning core a dynamical optically thick radiative envelope and an expanding atmosphere in which line acceleration is taken into account. The fitting procedure uniquely determines all the properties of the configuration, including the mass-loss rate $\dot{M}$ and the terminal velocity $v_\infty$, as a function of the total mass $M$. Although the bulk of the acceleration takes place in the atmosphere and is mainly due to line driving, dynamics is found to be not completely negligible even below the thermalization radius where only the gradients of isotropic radiation and gas pressure are responsible for acceleration. The derived values of $\dot{M}$ and $v_\infty$ are in good agreement with the observational data for Wolf-Rayet stars. In particular, the $\dot{M}$ versus $M$ relation derived by Abbott *et al.* for W-R stars in binary systems is well reproduced.

*Subject headings:* Stars: atmospheres — stars: mass loss — stars: winds — stars: Wolf-Rayet

## I. INTRODUCTION

Line-driven wind models (Castor, Abbott, and Klein 1975; Pauldrach, Puls, and Kudritzki 1986; hereafter CAK and PPK, respectively; Abbott 1982a; Friend and Castor, 1983; Friend and Abbott 1986) proved to be a very successful tool in explaining the observed properties of mass loss from OB stars.

Although the same acceleration mechanism could be, in principle, thought to work in Wolf-Rayet stars, which exhibit the highest rates of mass loss (see, e.g., the recent review by Chiosi and Maeder 1986), a straightforward application of the CAK theory to these stars is questionable for a number of reasons. In fact, as stressed by several authors (Abbott 1982a, b; Abbott and Lucy 1985; Pauldrach *et al.* 1985; Lucy 1986), the core-halo approximation is going to break down in the dense expanding envelopes of W-R stars, where optical depth unity in electron scattering is reached far away in the wind. Moreover, the chemical composition of W-R atmospheres, being enriched by nuclear burning products, is quite different from that of OB stars. While any increase in metallicity is not likely to alter deeply the efficiency of radiative acceleration (Abbott 1982a, b), the dynamical effects of continuum creation in the wind are not well investigated at present (see, however, Abbott and Lucy 1985). A further, and perhaps more important, source of uncertainty is the lack of reliable determinations of the stellar parameters in W-R stars. In particular, the use of commonly accepted values for luminosity and effective temperature in constructing wind models fails to explain the observed fact that W-R stars are $\sim 10$ times more efficient in converting radiative momentum into wind momentum than OB stars of comparable luminosity and temperature.

A possible conclusion is simply that the radiative force due to scattering of photons in the metal lines is not sufficient to produce the observed high $\dot{M}$ values, and, as a consequence, a different mechanism for wind acceleration is needed. An alternative possibility exists, however, and was recently suggested by Pauldrach *et al.* (1985) on the basis of parameters of the W-R binary V444 Cyg newly determined by Cherepashchuck Eaton, and Khaliullin (1984). According to these data, the commonly accepted values for the W-R star's effective temperatures and luminosity could be underestimated by a substantial amount, the observed values being in the range 80,000–100,000 K and $3$–$7 \times 10^5 \, L_\odot$, respectively. Assuming $L/L_\odot \approx 5.4 \times 10^5$, Pauldrach *et al.* (1985) succeeded in reproducing the observed wind parameters of V444 Cyg satisfactorily by means of radiative acceleration. Such high values of luminosity seem, however, difficult to reconcile with the predictions of stellar evolution, if one believes that W-R stars are the He-burning remnants of massive stars which have lost their hydrogen-rich outer envelope. The evolutionary tracks computed by Maeder (1983) show, in fact, that the luminosity of a $10 \, M_\odot$ remnant is $\sim 1.8 \times 10^5 \, L_\odot$, quite independently of the initial stellar mass and the assumed mass-loss rate, while the effective temperatures are indeed $\sim 100,000$ K.

Although one can argue that computed evolution of massive stars is not entirely trustworthy because the mass-loss rates are not self-consistently calculated, it is at the same time true that all the wind models computed up to now suffer from the fact, that, besides the stellar mass $M$, two input parameters must be supplied once a temperature distribution is chosen: the radius of the CAK critical point (or the photospheric radius) and the stellar luminosity. While this limitation is not too severe in the case of OB stars for which reliable data exist, it could introduce substantial errors for W-R stars, whose parameters are poorly known. These difficulties can be circumvented only by computing a model for the whole star which takes into account both

---

[1] Present address: Department of Physics, University of Padova, Italy.

the nuclear burning core and the radiatively expanding envelope.

In this paper we discuss how to construct such a unified model, and we present numerical results under some simplifying assumptions. We shall focus our attention on helium models which are chemically homogeneous and in which only central $3\alpha$ burning is present. They correspond to the He zero-age main sequence (ZAMS) which can be assumed as an idealized representation of W-R stars. Moreover, since principal goal of the present investigation is to test whether radiative acceleration can explain the main observed features of W-R winds, we shall further restrict ourselves to the quite over-simplified picture in which both the core halo and the radial streaming approximations hold; the possible effects of dropping these two crucial assumptions are discussed briefly in the last section. The computed models turn out to be completely characterized just by the total mass, all the other free parameters being fixed by the fitting between the three zones in which the structure is divided: a central hydrostatic convective core, a radiative dynamical envelope, and an atmosphere, which is optically thin with respect to true emission-absorption, where line driving is taken into account.

## II. BASIC EQUATIONS

In order to analyze better the various physical processes governing a dynamical model, it is more convenient to divide the stellar structure into three regions and discuss them separately. Such a division is made mainly in order to take into account the varying importance and different forms that dynamical terms assume in different stellar layers. In particular, we have chosen to distinguish: (a) a hydrostatic, convective core in which nuclear burning occurs; (b) a dynamical envelope, treated in the diffusion approximation, that extends up to the thermalization radius $r_*$ where the effective optical depth $\tau$ equals $\frac{2}{3}$; (c) a dynamical atmosphere where the contributions of both continuum and line scattering to radiative acceleration are taken into account.

### a) The Hydrostatic Core

Dynamics is certainly negligible in the central regions of the star, and, therefore, to avoid undue complications, we assume that the hydrostatic approximation describes our model there satisfactorily. In this limit the structure equations are just the usual equations governing static stellar models:

$$\frac{d \ln T}{d \ln r} = -\frac{(1 + 4a)}{5 + 8a(5 + 4a)} \frac{m}{rv_c^2} , \qquad (1)$$

$$\frac{d \ln \rho}{d \ln r} = \frac{3(1 + 8a)}{2(1 + 4a)} \frac{d \ln T}{d \ln r} , \qquad (2)$$

if the layer is convective or

$$\frac{d \ln T}{d \ln r} = -\frac{\Gamma}{8arv_c^2} , \qquad (3)$$

$$\frac{d \ln \rho}{d \ln r} = -\frac{1}{2rv_c^2} \left( m - \frac{1 + 4a}{4a} \Gamma \right) , \qquad (4)$$

if the layer is radiative. In both cases,

$$\frac{dm}{d \ln r} = 1.63 \times 10^{-16} M^2 \rho r^3 \qquad (5)$$

and

$$\frac{dl}{d \ln r} = \frac{dm}{d \ln r} \epsilon_{3\alpha} . \qquad (6)$$

Here $a = P_{rad}/P_{gas}$ is the radiation to gas pressure ratio, $v_c^2 = (\partial P/\partial \rho)_T = P_{gas}/\rho$ is the isothermal sound speed, $M$ is the total mass in unit of $M_\odot$, $m = M(r)/M$ is the fractionary mass, $l$ is the power emerging from a sphere of radius $r$, while all the other symbols have their usual meaning. The gas is assumed to be completely ionized helium obeying a perfect gas equation of state. The adimensional power generation rate per unit mass due to $3\alpha$ burning is

$$\epsilon_{3\alpha} = 5.506 \times 10^6 Y^3 \rho^2 f_{3\alpha} T_8^{-3} \exp(-43.2/T_8)$$

(see, e.g., Cox and Giuli 1968). The luminosity $l = L/(2.52 \times 10^{38} M)$ is in units of the Eddington luminosity referred to the electron scattering opacity $k_{es} = 0.2 \text{ cm}^2 \text{ g}^{-1}$, while $\Gamma = (k/k_{es})l$ is the radiative luminosity in terms of the local Eddington luminosity; it can, of course, vary even if the radiative flux is constant, depending on the Rosseland mean opacity $k$. The reader must also be warned that $r$ is in units of the gravitational radius $r_g = 2GM M_\odot/c^2$ and velocities are in units of light velocity. We are aware that the choice of such units could be confusing outside the realm of general relativity, but we feel nevertheless that the simplification they introduce in the formulae makes their use worthwhile. This will be even more evident when the hydrodynamical equations are analyzed. It should be noted, moreover, that the form we used for the hydrostatic equations is not the usual one. This is done essentially to ensure formal continuity with the hydrodynamical equations which are more naturally written using the density instead of the pressure as one of the independent variables.

### b) Expanding Radiative Envelope

Once the energy transport in the stellar layers begins to be radiative, we give up the hydrostatic assumption and start treating the full hydrodynamical problem. As a matter of fact, this requirement is even too stringent, since the configuration can be treated with a very high accuracy in the hydrostatic limit as long as $v \ll v_c$; this condition is fulfilled up to the outermost low-density layers. The choice of the radius at which dynamics begins to be nonnegligible is, in fact, somewhat arbitrary, although the fact that it is arbitrary is not crucial, and in the present case is suggested just by the fact that massive He-stars exhibit a completely convective core and an envelope which is radiative almost everywhere, apart from thin sub-photospheric layers. Here and in the following we will therefore identify the *core* as the central region extending up to the radius where radiative transport begins, while we will refer to the *envelope* as the intermediate zone up to effective optical depth $\tau = \frac{2}{3}$. Since LTE holds almost exactly below the thermalization radius, we can safely treat the envelope in the diffusion approximation.

The hydrodynamical equations for an optically thick medium were already discussed by several authors in connection with both outflowing stellar envelopes (e.g., Żytkov 1972; 1973) and models for X-ray bursters or classical novae (e.g., Ruggles and Bath 1979; Kato 1983; Quinn and Paczyński 1985; Joss and Melia 1986). A detailed analysis of the mathematical properties of the solutions was recently given by Turolla, Nobili, and Calvani (1986). Following their approach

the flow equations can be written in the nonrelativistic limit as

$$\frac{d \ln \rho}{d \ln r} = \frac{1}{2r(v^2 - v_c^2)}\left(m - \frac{1 + 4a}{4a}\,\Gamma - 4rv^2\right), \qquad (7)$$

or equivalently

$$\frac{d \ln v}{d \ln r} = \frac{1}{2r(v^2 - v_c^2)}\left(\frac{1 + 4a}{4a}\,\Gamma - m + 4rv_c^2\right), \qquad (7a)$$

$$\frac{dl}{d \ln r} = 3.41 \times 10^8\,\frac{(1 + 8a)(\dot{M}/M)}{2r(v^2 - v_c^2)}$$
$$\times \left[\frac{(v^2 - v_c^2)}{4a}\,\Gamma + v_c^2(\gamma_3 - 1)(m - 4rv^2)\right], \quad (8)$$

$$\rho vr^2 = 1.91 \times 10^3 \dot{M}M^{-2}, \qquad (9)$$

plus equations (3) and (5); the last one is still necessary as we push our dynamical integration deep into the stellar structure where the mass varies appreciably. The mass-loss rate $\dot{M}$ is expressed in $M_\odot$ yr$^{-1}$, while the adiabatic sound speed $v_s^2 = (\partial P/\partial \rho)_s$ and the third adiabatic exponent $\gamma_3$ are given by

$$v_s^2 = \frac{5 + 8a(5 + 4a)}{3(1 + 8a)}\,v_c^2; \qquad \gamma_3 = 1 + \frac{2(1 + 4a)}{3(1 + 8a)}.$$

The physical interpretation of the terms appearing in the momentum equation (7) is immediate, recalling that $m$ is related to the gravitational pull due to matter inside the sphere of radius $r$ while $(1 + 4a)\Gamma/4a$ accounts for both radiation and gas pressure forces. The correction $4rv^2$ arises as a consequence of spherical symmetry and is usually negligible. In the limit of vanishing flow velocity equation (7) reduces to the hydrostatic case (4). Equation (9) is the integrated mass conservation law, where $\dot{M}$ is a constant in the case of a stationary flow. Actually this is not rigorously true in our problem since the total mass is varying with time. We can nevertheless assume that the flow is stationary as long as the mass-loss time scale $M/\dot{M}$ is much longer than the dynamical time $\sim rr_g/vc$, a condition which is surely fulfilled for $\dot{M} < 10^{-4}\ M_\odot$ yr$^{-1}$ if $vc > 1$ cm s$^{-1}$; this value for the velocity is so low that it is not going to introduce any real constraint since the hydrostatic limit has been already met well before this.

Equation (8) describes the evolution of radiative luminosity under the assumption that no nuclear energy generation is present. We want to point out, moreover, that the dynamical energy equation does not yield equation (6) in the static limit. The reason is simply that we are dealing with two different physical processes for energy generation: nuclear reactions and conversion of internal energy into diffusive luminosity, the latter being effective only if a nonvanishing velocity field is present. In the limit $\dot{M} \to 0$ equation (8) gives constant luminosity, which agrees with equation (6) when $\epsilon_{3\alpha}$ is zero.

The dynamical equations show the presence of both critical and subcritical points which in general impose regularity constraints on the transonic solution (see Turolla, Nobili, and Calvani 1986 for details). In particular $\dot{M}$ turns out to be an eigenvalue of the problem once two input parameters (e.g., density and temperature at the critical radius) are specified. However, since we are dealing here only with a flow which is subsonic everywhere in the envelope, we do not need to bother about the existence of such regularity conditions.

## c) The Atmosphere

In the optically thick region the strong coupling between matter and radiation provides us with all the basic equations via the diffusion approximation. On the contrary, when the effective optical depth drops below unity, one has to face the much more difficult problem of solving the complete radiative transfer coupled with the hydrodynamical equations. Although possible in principle, such a task is so complicated that usually some simplifying assumptions are introduced. In particular, if one is mainly interested in studying the bulk properties of the wind, a common approach is to adopt a temperature distribution fixed a priori and to treat the matter-radiation interaction by means of a given sample of metal lines, actually ignoring the true evolution of the radiation field. Such a procedure, first introduced by Castor, Abbott, and Klein, proved very successful in explaining the observed properties of winds in OB stars, and it has the main advantage that all the interaction terms are grouped together in a single force multiplier.

Recently PPK extended CAK's work, dropping the radial streaming approximation and using also the more accurate expression for the force multipler given by Abbott (1982a). Although CAK's theory can be inadequate to describe W-R star winds in view of the possible failure of the core-halo hypothesis, we shall nevertheless assume that both the core halo and the radial streaming approximations hold. A discussion about this point is postponed to the last section.

CAK's momentum equation can be cast in our notation as

$$\frac{d \ln v}{d \ln r} = \frac{1}{2r(v^2 - v_c^2)}\left[(1 + \mathscr{M})\Gamma - 1 + 4rv_c^2\left(1 - \frac{d \ln T}{d \ln r}\right)\right], \qquad (10)$$

where we have put $m = 1$, the contribution of the atmosphere to the total mass being completely negligible. The force multiplier $\mathscr{M}$ takes into account the scattering of photons into Doppler-broadened metal lines and formally enters the Euler equation as an extra contribution to the total opacity (see eq. [7a] for comparison). The multiplier $\mathscr{M}$ is well approximated by a power-law fit to the tabulated values (CAK; Abbot 1982a)

$$\mathscr{M} = K\left(\frac{n_e}{W}\right)^\delta t^{-\alpha}, \qquad (11)$$

where $K$, $\alpha$, and $\delta$ can be regarded as constants, $n_e$ is the electron density in units of $10^{11}$ particles cm$^{-3}$, $W = \{1 - [1 - (r_*/r)^2]^{1/2}\}/2$ is the dilution factor,

$$t = 2.96 \times 10^5 Mk_{es}\,\rho r\left(\frac{v_{th}}{v}\right)\left|\frac{d \ln v}{d \ln r}\right|^{-1} \qquad (12)$$

is the line optical depth in an expanding medium and $v_{th}$ is the thermal velocity of the scattering ions (see CAK and PPK for details).

Equation (10) must be supplemented with the continuity equation (9) and a temperature distribution $T = T(r)$, which is an input parameter as no energy equation is solved. It is interesting to note that if an energy balance is specified, it is possible to eliminate the temperature gradient from the momentum equation (10), and this in turn changes the critical velocity to the adiabatic sound speed. Although not particularly relevant in the present case (since the isothermal sound speed is not the real critical velocity in eq. [10] because of the dependence on the velocity gradient in $\mathscr{M}$), one should keep in mind that, in general, the sonic point in an optically thin flow is associated

with the adiabatic sound speed and not with the isothermal one, as discussed by Turolla, Nobili, and Calvani (1986).

The momentum balance equation (10) is a nonlinear equation in $d \ln v/d \ln r = v'$ and can be written explicitly as

$$(v^2 - v_c^2)v' - CG(r)v^{2\alpha - \delta}(v')^{\alpha} + H(r) \equiv F(r, v, v') = 0 , \quad (13)$$

with

$$G(r) = 2^{\alpha - 1}W^{-\delta}r^{-2\delta} , \quad (14)$$

$$H(r) = \frac{1 - \Gamma}{2r} - 2v_c^2\left(1 - \frac{d \ln T}{d \ln r}\right) , \quad (15)$$

and

$$C = K\Gamma\left(\frac{8.82 \times 10^{-10}}{k_{es}v_{th}}\right)^{\alpha}\left(\frac{5.61 \times 10^{15}}{M}\right)^{\delta}\left(\frac{M}{\dot{M}}\right)^{\alpha - \delta} . \quad (16)$$

As it was proved by CAK, the equation $F(r, v, v') = 0$ may admit zero, one, or two solutions according to the values of $r$ and $v$. The requirement that a continuous solution for $v'$ exists in the whole domain $r_* < r < \infty$ and $v(r_*) < v < v_\infty$ implies that the two conditions

$$\frac{\partial F(r, v, v')}{\partial v'} = 0 , \qquad \frac{dF(r, v, v')}{d \ln r} = 0 , \quad (17)$$

must be satisfied at $r_{CAK}$ (the CAK critical point). The existence of the constraints (17) fixes the eigenvalue $\dot{M}$, the flow velocity, and its derivative at the CAK point. The latter is the positive solution of the quadratic equation

$$(v')^2 + \frac{\delta H(r)}{2v_c^2(1 - \alpha)}v' - \frac{H(r)}{2v_c^2}\left[\frac{1}{(1 - \alpha)}\frac{d \ln G}{d \ln r} - \frac{d \ln H}{d \ln r}\right] = 0 ,$$

$$(18)$$

$$v_{CAK}^2 = v_c^2 + \frac{\alpha}{(1 - \alpha)}\frac{H(r)}{v'_{CAK}} , \quad (19)$$

while $\dot{M}$ follows from the previous definition of $C$ and from

$$C = \left.\frac{(v^2 - v_c^2)(2rv')^{1-\alpha}}{\alpha G(r)v^{\alpha - \delta}}\right|_{CAK} . \quad (20)$$

These expression differ from the classical CAK results since we have also taken into account the dependence on the electron density in the force multiplier. They can also be directly derived from PPK assuming radial streaming of photons in their equations

### III. DYNAMICAL STELLAR MODELS

The numerical integration of the ordinary hydrostatic stellar structure equations, normally performed by means of Henyey's method, yields a unique solution once the usual boundary conditions are specified together with the total mass. In particular, the overall stellar properties are quite insensitive to the photospheric boundary conditions so that even the *zero boundary conditions* give a reasonable approximation.

On the contrary, photospheric properties play a crucial role in dynamical models. The whole wind structure, and consequently the mass-loss rate, in fact strongly depends on the photospheric conditions. The need for an accurate computation of the outermost stellar layers, the appearance of a critical point, and the presence of different physical regimes in different stellar regions make it more difficult to deal with the complete dynamical problem. One of the major complications lies in the fact that the search for an eigenvalue requires both a piecewise integration and matching among the various parts of the solution in order to satisfy the boundary as well as the critical point conditions.

The basic scheme is as follows: the numerical integration is carried out starting from the center until a given value of the fractionary mass is reached; the same is done integrating from the CAK critical point inward. The matching of the two branches of the solution fixes all the unknown parameters with the exception of one which, in our case, is the optical depth at the critical point $\tau_{CAK}$. The latter is then determined requiring that the boundary condition $\tau = 0$ is fulfilled for $r \rightarrow \infty$. Once convergence is attained, a model is fully characterized only by the total mass of the configuration in an analogous way to what Voigt-Russell theorem predicts for static structures.

The first part of the integration is performed by means of the hydrostatic equations (1)–(6), recast using the mass parameter $q = \ln [m/(1 - m)]$ as the independent variable. This is commonly done in stellar evolution calculations, since it is the more suitable form for numerical integration. The standard central boundary conditions $m(0) = 0$, $l(0) = 0$ are replaced, again for numerical convenience, by specifying all the quantities at the surface of a homogeneous kernel containing a small fraction of the mass $m_0$ ($m_0 = 10^{-2}$ in the actual models). Denoting the central density and temperature by $\rho_c$ and $T_c$, respectively, the initial conditions are

$$q_0 = \ln [m_0/(1 - m_0)] , \quad r_0 = 2.63 \times 10^5(m_0 M^{-2}\rho_c^{-1})^{1/3} ,$$

$$\ln T_0 = \ln T_c - \frac{1 + 4a}{5 + 8a(5 + 4a)}\frac{m_o}{3r_0 v_c^2} ,$$

$$\ln \rho_0 = \ln \rho_c - \frac{1 + 8a}{5 + 8a(5 + 4a)}\frac{m_o}{2r_0 v_c^2} , \qquad l_0 = (\epsilon_{3\alpha})_c m_0 ,$$

where the thermodynamical quantities $a$ and $v_c^2$ are evaluated at the center. Given an initial guess for the central values of density and temperature, the integration can be started at $q_0$ and carried out to the fitting point $q_f$ (we have chosen the corresponding value of $m_f$ in the range 0.75–0.85). Since the location of the last convective layer is not known *a priori*, we found it to be more convenient to switch on dynamics only after the fitting point is reached and not when radiative transport begins. This will not introduce any error, according to the discussion in the last section. As a consequence, our models will have a static radiative zone described by equations (3) and (4). The structure starts to be radiative when Schwarzschild criterion is satisfied; that is to say, using our notation, when

$$\frac{8a(1 + 4a)}{5 + 8a(5 + 4a)}\frac{m}{\Gamma} \geq 1 .$$

The next step is to integrate from the CAK critical point inward, using equations (9) and (10) and specifying a temperature distribution. Because the wind dynamics is quite insensitive to the temperature profile in the atmosphere (see CAK and PPK), we use a simple gray temperature distribution:

$$T^4 = \frac{3}{4} T_{eff}^4\left(\tau + \frac{2}{3}\right) , \quad (21)$$

where $T_{eff}$ is the effective temperature at the thermalization radius. Defining an effective opacity coefficient $k_* =$

$[3k(k - k_{es}]^{1/2}$, where $k$ is the Rosseland mean opacity, and denoting the dimensional radius by $\xi$, the effective optical depth is, in spherical symmetry,

$$\tau = -\int_{\xi}^{\infty} k_* \rho \left(\frac{r_*}{r}\right)^2 d\xi . \qquad (22)$$

The choice of the optical depth as the integration variable is here the most natural one, so we need to add the differential form of equation (22):

$$\frac{d \ln r}{d\tau} = -\frac{3.37 \times 10^{-6}}{k_* M\rho} \left(\frac{r}{r_*}\right)^2 \qquad (23)$$

to equations (9) and (10).

In order to start the integration of the atmosphere, we need a value of the thermalization radius $r_*$ which enters both the definition of $W(r)$ and equation (23), but unfortunately $r_*$ can be evaluated only after the integration has reached $\tau = \frac{2}{3}$. To overcome this difficulty and since $r_*$ is just below the critical radius (PPK), one can tentatively assume that $r_* = r_{CAK}$. The exact value of $r_*$ will then be computed within an iterative loop (see below). All the quantities at the critical point and the eigenvalue $\dot{M}$ can now be evaluated, using the regularity conditions at $r_{CAK}$, once trial values for $r_{CAK}$ and for $l(r_{CAK})$ are given together with a first guess for $\tau_{CAK}$, if one neglects temperature derivatives in equations (18) and (20). The values of $\dot{M}$ and $v_{CAK}$ can be then improved through successive iterations, using for the temperature derivatives the expressions

$$\frac{d \ln T}{d \ln r} = -\frac{1.42 \times 10^8}{(\tau + 2/3)} \frac{\dot{M}}{M} \frac{k_*}{rv} \left(\frac{r_*}{r}\right)^2 , \qquad (24)$$

and

$$\frac{d^2 \ln T}{d \ln r^2} = -\frac{d \ln T}{d \ln r} \left(4 \frac{d \ln T}{d \ln r} + \frac{d \ln v}{d \ln r} + 3\right), \qquad (25)$$

which follow from equations (21) and (23) after eliminating $\rho$ via the continuity equation and with the assumption of constant opacity in deriving equation (25). We would like to stress that in any case these terms are not going to introduce substantial corrections in the computed values of $\dot{M}$ and $v_{CAK}$. Equations (9), (10), and (23) are now integrated up to $\tau = \frac{2}{3}$ which we assume to be the border of the optically thick region. From $r_*$ inward they are replaced by equations (7)–(9), rewritten using $\ln \rho$ instead of $\ln r$ as the independent variable, and the integration is carried on until the fitting point is reached.

The four unknown parameters $\rho_c$, $T_c$ (relative to the inner solution), $l(r_{CAK})$, $r_{CAK}$ (defining the outer one) are evaluated by means of a standard shooting plus Newton iteration technique. The inner integration is performed 3 times: the first one using the trial values $\rho_c$, $T_c$, then varying $\rho_c$ (at fixed $T_c$), and finally varying $T_c$ (at fixed $\rho_c$). The same procedure applies to the outer integration, perturbing now $l(r_{CAK})$ and $r_{CAK}$. These trial integrations are used to compute partial derivatives of the discontinuities at the fitting point with respect to the values of the trial parameters. More accurate starting conditions are then interpolated from these derivatives, assuming that all the jumps vanish at the fitting point, and the whole scheme is iterated until convergence is achieved.

The model computed in this way contains nevertheless a free parameter, since the optical depth at the critical point still needs to be fixed. This indetermination is just a consequence of the lack of boundary conditions at infinity and can be removed

once the correct constraint is imposed, assuming that $\tau = 0$ as $r \to \infty$. In order to do that we have used again a shooting method, varying $\tau_{CAK}$ and integrating equations (9), (10), and (23) up to some fiducial radius $r_\infty$ which represent radial infinity. For all practical purposes one can assume $r_\infty = 50 r_{CAK}$, since both $v$ and $\tau$ have attained their asymptotic values there.

The construction of one model can therefore be thought as divided into a large loop in which $\tau_{CAK}$ is varied and a small loop in which a self-consistent *internal* solution is generated for each value of $\tau_{CAK}$. Convergence proved not to be critical provided that reasonable starting values for $\rho_c$, $T_c$, $r_{CAK}$ and $l(r_{CAK})$ are given. Usually most of the computing time is spent achieving convergence within the small loop the first time it is entered, since the variations in $\tau_{CAK}$ do not influence deeply the interior structure.

IV. NUMERICAL RESULTS

The integration method developed in the last section is applied here to compute a sequence of dynamical stellar models for different masses. Since the observed masses of W-R stars lie mainly in the range $10\ M_\odot \lesssim M \lesssim 20\ M_\odot$ (Massey 1982), we selected three representative values in this inverval for numerical integrations: $M = 10\ M_\odot$ (model A), $M = 15\ M_\odot$ (model B), and $M = 20\ M_\odot$ (model C). Model A has a special significance since it provides us both with a direct comparison with the existing observational data for V444 Cyg and with a check with previous theoretical results obtained by Pauldrach *et al.* (1985) for the wind structure of this star.

All the integrations were performed using Cox and Stewart's (1970) opacity tables referring to a mixture of composition $X = 0$, $Y = 0.98$, and $Z = 0.02$. In order to avoid the presence of discontinuities in the opacity gradients, which turn out to be quite troublesome in the dynamical part of the code, a bicubic spline interpolation to the tabular values of opacity was used. A major open problem is the choice of the constants $K$, $\alpha$, and $\delta$ appearing in the expression for the force multiplier (eq. [11]). The tabulation given by Abbott (1982a) and mainly aimed to OB stars winds stops, in fact, at $T_{eff} = 50,000$ K, while the effective temperature of W-R stars can be a factor or 2 higher. Moreover, $K$ shows quite a strong dependence on the electron density in the atmosphere, so one is in the uncomfortable position of extrapolating (or, really, guessing) the appropriate values starting from very poor information. Pauldrach *et al.* (1985) used $K = 0.137$, $\alpha = 0.68$, and $\delta = 0.07$, claiming that they represent well the hot boundary of Abbott's table, although some of their models are computed with $K = 0.177$ and $\delta = 0.02$. These values are indeed the hot boundary but with the tacit assumption that the parameter $(n_e/W)$ is in the range $3.1 \times 10^8 \leq (n_e/W) \leq 3.1 \times 10^{11}$; that is to say, they are using the low-density limit of the force multiplier log. It should be stressed, however, that the central value (out of three) of $n_e/W$ used in Abbott's tabulation *is estimated to typify the winds of OB stars* and can therefore poorly represent W-R stars winds, which are commonly thought to be much denser. Following this reasoning, we have decided to use as fiducial values $K = 0.42$, $\alpha = 0.65$, and $\delta = 0.09$. They represent the hot boundary, assuming that $(n_e/W)_{W-R} \approx 100(n_e/W)_{OB}$, and which were obtained from Abbott's data, considering that $K$ depends weakly on temperature and more strongly on density, the contrary holding for $\alpha$. The validity of this assumption can, of course, be checked a posteriori by looking at the value of $n_e/W$ computed by the code. We are, in any case, aware that our

TABLE 1
PARAMETERS OF CALCULATED MODELS

| Model | $M/M_\odot$ | $R_s/R_\odot$ | $R_*/R_\odot$ | $T_{eff} \times 10^{-5}$ | $L/L_\odot \times 10^{-5}$ | $\Gamma$ | $\rho_s \times 10^{11}$ (g cm$^{-3}$) | $\dot{M} \times 10^5$ $M_\odot$ yr$^{-1}$ | $v_\infty$ (km s$^{-1}$) | $\dot{M}v_\infty c/L$ |
|---|---|---|---|---|---|---|---|---|---|---|
| A......... | 10 | 1.09 | 0.88 | 1.13 | 1.37 | 0.21 | 7.94 | 0.85 | 2330 | 7.14 |
| B......... | 15 | 2.44 | 1.11 | 1.22 | 2.93 | 0.30 | 2.40 | 2.41 | 2410 | 9.82 |
| C......... | 20 | 4.40 | 1.30 | 1.28 | 4.82 | 0.37 | 1.26 | 4.72 | 2450 | 12.0 |

choice is just tentative, and the consequences of modifying these values will be discussed later on.

The main parameters characterizing each model are shown in Table 1. The radius $R_s$ appearing there corresponds to the last scattering surface defined by $\tau_{es} = \frac{2}{3}$ and $\rho_s = \rho(R_s)$. The computed values of $\dot{M}$ and $v_\infty$ show a good general agreement with the observational data recently reviewed by Abbott et al. (1986). The agreement between the observed and the computed terminal velocities must, however, be taken with care, since it is known that the radial streaming approximation can underestimate $v_\infty$ by a factor of 2–3 in the case of OB stars (PPK; Friend and Abbott 1986). It is interesting to compare our theoretical predictions with observations in the case of the sample of the five binary W-R stars considered by these authors and for which a fairly good mass estimate exists. The tentative $\dot{M}$ versus $M$ relation obtained in their paper and yielding $\dot{M} \propto M^{2.3}$, is, in fact, reproduced almost exactly by our calculations, which give a linear relation between log $\dot{M}$ and log $M$, in the mass range considered, with a slope of 2.4. The derived relation is plotted in Figure 1, together with the observational data and their linear best fit. Figure 1 seems, nevertheless, to suggest that the computed values of $\dot{M}$ are systematically underestimated, although not by a substantial amount. It is interesting to note, however, that other numerical integrations performed with different values of $K$ and $\alpha$ show the same scaling law for $\dot{M}$: the net result is just to shift up or down the full line in Figure 1. The overall variation in $\dot{M}$ is within a factor of 5, if $K$ and $\alpha$ are chosen at the hot boundary of Abbott's table.

This remarkable feature is not surprising since, in CAK's theory, $\dot{M}$ depends on the mass both in an explicit and in an implicit way, through $\Gamma$. In other words, it is the mass-luminosity dependence which determines the form of the $\dot{M}$ versus $M$ relation rather than any other effect. In particular, the fact that our models follow such a relation is quite indepen-

dent on the details of the radiative interaction in the wind, and it strengthens the suggestion of Abbott et al. that this correlation should hold for all W-R stars in the mass interval here considered. We note, however, that for $M \lesssim 10\ M_\odot$ our models predict a gradual steepening in the dependence of $\dot{M}$ on stellar mass, as it is apparent from Figure 1 where only the 7 $M_\odot$ model is explicitly shown. On the other hand, according to our calculations, for $M \gtrsim 25\ M_\odot$, the flow becomes supersonic well below the thermalization radius. Most probably this is just a consequence of the complete failure of the core-halo approximation, which is less and less reliable in modeling the flow for increasing stellar masses (see the discussion in § V).

Contrary to what happens for the mass-loss rate, data in Table 1 do not support any strong correlation between terminal velocity and mass, luminosity, or radius; $v_\infty$ is, in fact, fairly constant, although a weak dependence on $M$ is present. We note also that the derived values of $\dot{M}v_\infty c/L$ ($v$ is here in ordinary units), which is the ratio of wind momentum to radiative momentum, are of the order of 10, as is observed in W-R stars.

The runs of velocity and density versus radius are plotted in Figures 2a and 2b, respectively, for model A. Figure 2a shows clearly that the bulk of the acceleration takes place beyond the thermalization radius, being due mostly to line driving. Radiative acceleration is, however, not entirely negligible even in the optically thick region since the velocity at $r_*$ is $\sim 5$ km s$^{-1}$. Both the velocity and the density profiles are qualitatively very similar to those ones computed by Pauldrach et al. as far as the wind zone is concerned, although some quantitative differences are present. These discrepancies seem to be due mainly to the different values of luminosity and radius we obtained from our stellar structure calculations, rather than to the different parameterization of $\mathscr{M}$. We note, however, that, despite the use of quite crude approximations in treating the wind region, model A does succeed in reproducing the most important features of V444 Cyg wind, thus providing us with further evidence in favor of line driving as the basic acceleration mechanism in W-R stars.

## V. DISCUSSION AND CONCLUSION

The results reported in the last section suggest that the basic observed properties of W-R stars can be reproduced assuming that they are homogeneous helium structures undergoing central $3\alpha$ burning and invoking line acceleration as the main driving force in their extended atmospheres. Although our models still need improvement, we feel that they can nevertheless be used as a starting point for future work.

As we have stressed before, the main limitations of our approach, besides the uncertainties in the force multiplier, come from retaining the core-halo approximation in our treatment of the wind dynamics and from having used a chemically homogeneous helium structure to describe a W-R star. Let us discuss these two points separately.

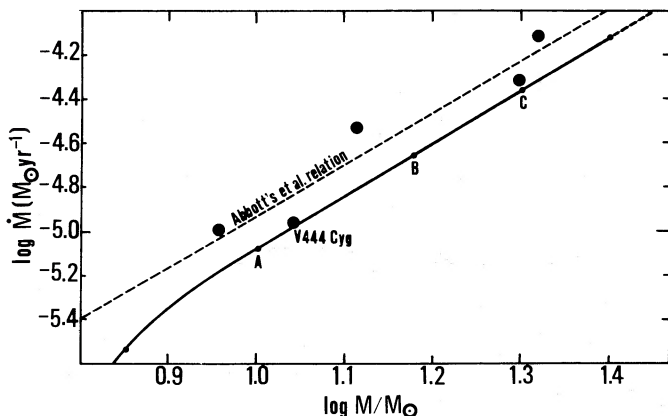One of the major objections to the applicability of the CAK



FIG. 1.—Derived $\dot{M}$ vs. $M$ relation (solid line) compared to the observational data (large dots) and their linear best fit (dashed line) as taken from Abbott et al. (1986). Small dots represent computed models.
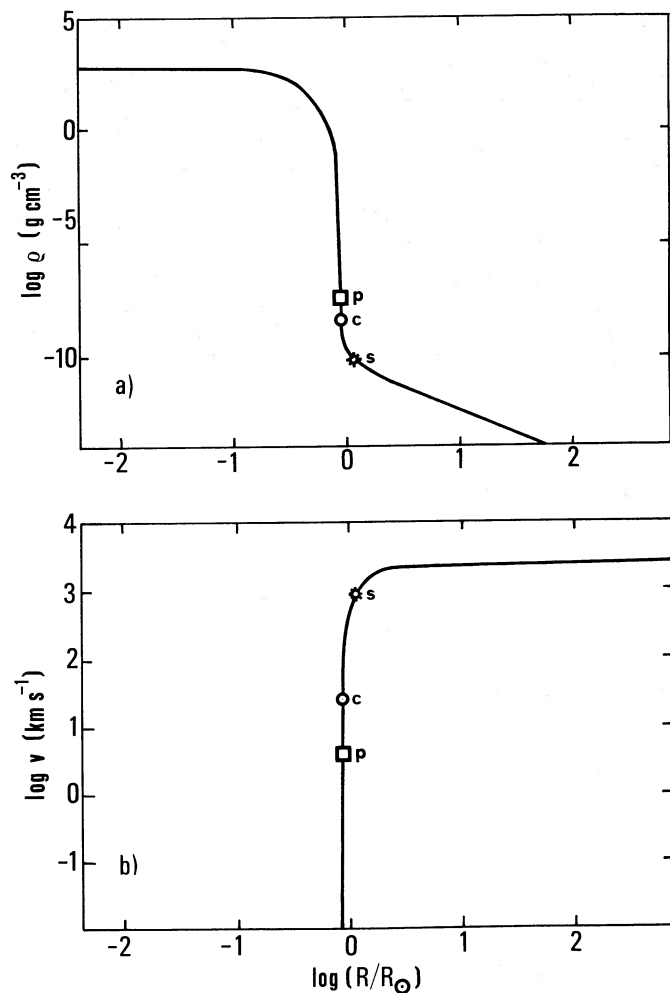
FIG. 2.—(a) Run of density vs. radius for model A. The points labeled P, C, and S show the locations of the photosphere, the sonic point, and the last scattering surface, respectively. (b) Run of velocity vs. radius.

theory to W-R stars is that line driving is thought to be quite inefficient to accelerate the flow in the wind dense inner region where the radiation field is nearly isotropic. More precisely, this effect can be important in the zone in between the two radii at which electron scattering optical depth and effective optical depth equal $\frac{2}{3}$, $r_s$ and $r_*$, respectively. In fact, below $r_*$ diffusion approximately holds, so that the concept itself of force multiplier is meaningless and equations (7)–(9) describe appropriately the flow dynamics there, while above $r_s$ the radiation field is almost radially streaming and consequently CAK approach is justified.

Clearly what one expects to happen for $r_* < r < r_s$ is that the force multiplier should be more and more depressed approaching $r_*$, owing to the increasing degree of isotropy of the radiation field.

To get more insight on the influence of this effect on the wind dynamics, let us suppose that the quantity $K$, defined in equation (11), contains a damping factor, decreasing with increasing electron scattering optical depth. Formally this factor can be included in the definition of $G(r)$ and produces an increase in the magnitude of the velocity gradient at the CAK point and consequently a decrease of $v_{CAK}$, as can be seen from equations (18) and (19). As long as the damping is effective at

$r_{CAK}$ and $v_{CAK} \gg v_c$, $\dot{M}$ will be reduced with respect to the value computed with the core-halo approximation, being proportional to $K$. The most crucial point, for the internal consistency of our models, is that $\tau_{es}(r_{CAK}) \lesssim 1$ since $\dot{M}$ and $v_{CAK}$ are computed using the critical point conditions (17), which strictly hold only assuming a core-halo model. If this condition is fulfilled, the fact that the force multiplier is damped by back-scattered photons below the critical point does not preclude the possibility of accelerating the wind. The correct solution will differ from the CAK one, below the CAK radius, essentially for the velocity profile, which becomes steeper. The dynamical subphotospheric layers, which are governed by equations (7)–(9), are, however, elastic enough to react to all the changes in the outermost wind zone, and only the deep, and very dense, stellar region is really insensitive to the presence of the wind.

An estimate of how a damping of the force multiplier influences the wind parameters was obtained numerically, producing some test runs with the assumption that $K$ contains a damping factor proportional to exp $(-b\tau_{es})$ and modifying accordingly the critical point conditions following from equation (17). The computed solutions show substantial differences with respect to the previous ones as far as the terminal velocity is concerned. In the case of model B, in fact, with $b = 1$, we found $v_\infty = 5860$ km s$^{-1}$ and $\dot{M} = 1 \times 10^{-5}$ $M_\odot$ yr$^{-1}$. The effects of the damping term are therefore quite similar to those ones introduced by the finite disk correction: $v_{CAK}$ moves closer to the sound speed, $v_\infty$ increases while $\dot{M}$ is reduced. It should be stressed, however, that such a damping factor most probably overestimates the real effect of the progressive isotropization of the radiation field with increasing electron scattering optical depth. For smaller values of $b$ the increase in the terminal velocity is no longer so drastic: using $b = 0.2$ the computed terminal velocity is $\sim 3500$ km s$^{-1}$, which should be compared to the unperturbed value of $\sim 2500$ km s$^{-1}$.

The second point we would like to discuss concerns the chemical homogeneity assumption. Strictly speaking, one can not neglect the past evolution of the configuration in constructing more sophisticated models, simply because the evolution of a massive star with mass loss will produce a remnant which is not a pure helium star. Evolutionary tracks of this kind were recently computed by Maeder (1983), assuming an ad hoc mass-loss rate. The evolution was followed from the main sequence to the appearance of a nondegenerate core through the stages corresponding to blue supergiants and Hubble-Sandage varables. A comparison of the properties of the final, envelope-free, configurations, which are likely to represent W-R stars, with our models shows that luminosity is systematically $\sim 20\%$–30% lower in our case, for a given mass. This discrepancy cannot be due simply to our dynamical treatment or to differences in the numerical technique but must be related to more physical causes. As already stressed by Maeder, in fact, the overluminosity of W-R, compared to helium stars, arises as the consequence of the enrichment of their chemical composition by $3\alpha$ products which start to be formed before the W-R phase. Since the mass-loss rate goes roughly as $\dot{M} \propto (1 - L)^{-(1-\alpha)/\alpha}L^{-1/\alpha}$, an increase in luminosity, driven by the change in the mean molecular weight, will also produce an increase in $\dot{M}$ and consequently a shift of the full line in Figure 1 upward. It is interesting to note therefore, that taking into account evolutionary effect could explain that fact that our log $\dot{M}$ — log $M$ relation seems to be a lower limit to the observed values of the mass-loss rate.

In order to check the validity of these considerations we have computed again a 10 $M_\odot$ model varying the chemical composition. We have considered two cases in which the central carbon abundance was $X_c(^{12}C) = 0.1$ and $X_c(^{12}C) = 0.3$, respectively. The whole set of equations discussed in § II was modified to take into account for the gradient in the chemical composition; a profile for $X(^{12}C)$ as a function of $m$ was then specified, keeping $X(^{12}C) = X_c(^{12}C) = $ constant up to $m = 0.85$ and imposing the condition that it goes rapidly to zero for increasing fractionary mass. For simplicity (and lacking a better one) the opacity we used was still that of a mixture with $Y = 0.98$, $Z = 0.02$. This procedure was followed to mimic, as closely as possible within the limitation of our code, the structure of a 10 $M_\odot$ remnant as resulting from a evolution with mass loss. The results of these integrations suggest that the deficit in the mass-loss rate previously reported could be probably due to the initial assumption of chemical homogeneity. The model with $X_c(^{12}C) = 0.3$ gives in fact a luminosity which is $\sim 15\%$ higher with respect to model A, and the corresponding mass-loss rate is $\dot M = 1.15 \times 10^{-5} M_\odot$ yr$^{-1}$.

It should, be stressed, however, that, despite the good agreement of our models with observations, our results were obtained using both some simplifying assumptions in treating the wind dynamics and force multiplier parameters derived with a crude extrapolation of Abbott's data. Any progress in modeling W-R star winds will therefore demand an extension of the available line data at higher effective temperatures and a better parameterization of the force multiplier itself, which should take into account for departures from the core-halo approximation.

Further refinements in the present models can be obtained once the real chemical composition of the star and its spatial gradient are known; this can be done only including the computation of the mass-loss rate outlined in the present paper in a stellar evolutionary code. Although we have dealt here only with the problem of mass loss from W-R stars, our approach can nevertheless be applied also to OB stars, so that it would be possible in principle to follow the evolution of massive stars starting from the main sequence up to the W-R phase, without introducing any ad hoc assumption about the rate of mass loss. However, even such a hypothetical code will not be the final tool in stellar evolution since the present treatment is going to fail when the model enters a cooler giant phase. Mass loss in such stages is in fact not necessarily driven by radiative acceleration, and, most probably, other mechanisms, like shock waves, are at work (see, e.g., Castor 1981).

## REFERENCES

Abbott, D. C. 1982a, Ap. J., **259**, 282.
————. 1982b, in IAU Symposium 99, Wolf-Rayet Stars: Observations, Physics, Evolution, ed. C. W. H. de Loore, and J. Willis (Dordrecht: Reidel), p. 185.
Abbott, D. C., Bieging, J. H., Churchwell, E., and Torres, A. V. 1986, Ap. J., **303**, 239.
Abbott, D. C., and Lucy, L. B. 1985, Ap. J., **288**, 679.
Castor, J. I. 1981, in Physical Processes in Red Giants, ed. I. Iben and R. Renzini (Dordrecht: Reidel), p. 285.
Castor, J. I., Abbott, D. C., and Klein, R. I. 1975, Ap. J., **195**, 157 (CAK).
Cherepaschuk, A. M., Eaton, J. A., and Khaliullin, Kh. F. 1984, Ap. J., **281**, 774.
Chiosi, C., and Maeder, A. 1986, Ann. Rev. Astr. Ap., **24**, 329.
Cox, A. N., and Stewart, J. N. 1970, Ap. J. Suppl., **19**, 261.
Cox, J. P., and Giuli, R. T. 1968, Principles of Stellar Structure (New York: Gordon and Breach).
Friend, D. B., and Abbott, D. C. 1986, Ap. J., **311**, 701.
Friend, D. B., and Castor, J. I. 1983, Ap. J., **272**, 259.
Joss, P. C., and Melia, F. 1986, preprint.

Kato, M. 1983, Pub. Astr. Soc. Japan, **35**, 33.
Lucy, L. B. 1986 in IAU Colloquium 89, Radiation Hydrodynamics in Stars and Compact Objects, ed. D. Mihalas and K.-H. A. Winkler (Berlin: Springer-Verlag), p. 75.
Maeder, A. 1983, Astr. Ap., **120**, 113.
Massey, P. 1982, in IAU Symposium 99, Wolf-Rayet Stars: Observations, Physics, Evolution, ed. C. W. H. de Loore and J. Willis (Dordrecht: Reidel), p. 251.
Pauldrach, A., Puls, J., Hummer, D. G., and Kudritzki, R. P. 1985, Astr. Ap., **148**, L1.
Pauldrach, A., Puls, J., and Kudritzki, R. P. 1986, Astr. Ap., **164**, 86 (PPK).
Quinn, T., and Paczyński, B. 1985, Ap. J., **289**, 634.
Ruggles, C. L. N., and Bath, G. T. 1979, Astr. Ap., **80**, 97.
Turolla, R., Nobili, L., and Calvani, M. 1986, Ap. J., **303**, 573.
Żytkov, A. 1972, Acta Astr., **22**, 103.
————. 1973, Acta Astr., **23**, 121.

MASSIMO CALVANI: Department of Astronomy, University of Padova, Vicolo dell' Osservatorio, 35122 Padova, Italy

LUCIANO NOBILI and ROBERTO TUROLLA: Department of Physics, University of Padova, Via Marzolo 8, 35131 Padova, Italy